

1 **Supporting Information**

2

3 **Natriuretic peptide type C induces sperm attraction for fertilization in mouse**

4

5 Nana Kong<sup>1</sup>, Xiaoting Xu<sup>1</sup>, Yu Zhang<sup>1</sup>, Yakun Wang<sup>1</sup>, Xiaoqiong Hao<sup>1</sup>, Yu Zhao<sup>1</sup>,  
6 Jie Qiao<sup>2</sup>, Guoliang Xia<sup>1</sup> and Meijia Zhang<sup>1,\*</sup>

7

8 <sup>1</sup>State Key Laboratory for Agrobiotechnology, College of Biological Sciences, China  
9 Agricultural University, Beijing 100193, China. <sup>2</sup>Department of Obstetrics and  
10 Gynecology, Reproductive Medical Center, Peking University Third Hospital, Beijing  
11 100191, China.

12

13 N.K. and X.X. contributed equally to this work.

14

15 Correspondence: Meijia Zhang, State Key Laboratory for Agrobiotechnology, College  
16 of Biological Science, China Agricultural University, Beijing 100193, China. Tel: 86  
17 10 6273 2694. E-mail: zmeijia@cau.edu.cn.

18

19 **Table S1. Compare of sperm motility in NPR2 heterozygote and mutant mice**

Treatment	NPR2 heterozygote	NPR2 mutant
Progressive (%)	21.3 ± 1.3	19.4 ± 0.7
VAP (µm/s)	113.1 ± 2.4	116.2 ± 4.2
VSL (µm/s)	74.2 ± 2.1	76.6 ± 4.9
VCL (µm/s)	214 ± 6.6	223.3 ± 5.5
ALH (µm)	8.9 ± 0.4	8.5 ± 0.2
BCF (HZ)	25.2 ± 0.9	23.9 ± 0.6
STR (%)	61.8 ± 1.4	63.9 ± 0.6
LIN (%)	35.2 ± 1.2	36.4 ± 0.5

20

21 VAP, average path velocity; VSL, straight line velocity; VCL, curvilinear velocity;  
 22 ALH, amplitude of lateral head displacement; BCF, beat cross frequency; STR,  
 23 percentage of straightness; LIN, percentage of linearity; progressive motility (% of  
 24 motile spermatozoa with VAP ≥ 50 µm/s and STR ≥ 80%). Bars indicate the mean ±  
 25 SEM of three experiments; *n* = 500 for each sample.

26

27 **Table S2. Sequence of PCR primers used for qRT-PCR**

28

Primer	Forward	Reverse
<i>Nppa</i>	CCAGGCCATATTGGAGCAAAT	TTCTCCTCCAGGTGGTCTAGCA
<i>Nppb</i>	AGCTGCTTTGGGCACAAGAT	CAGGCAGAGTCAGAACTGGAGTCT

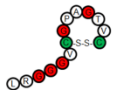

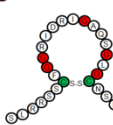

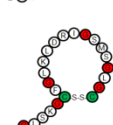
29

30

31

32 **Fig. S1. Comparison of amino sequences of mouse natriuretic peptides (NPs) and**  
 33 **the confirmed chemoattractants.** Amino acid sequence analysis revealed that mouse  
 34 natriuretic peptide type A (NPPA), type B (NPPB) and type C (NPPC) exhibited  
 35 similar characters to the chemoattractant peptides resact and asterosap in marine  
 36 invertebrates: there are glycine-rich peptides (red), circular by the formation of an  
 37 intramolecular disulfide bond between cysteines (green), and binding to a  
 38 receptor-type guanylyl cyclase (GC) to stimulate the synthesis of cGMP.

39

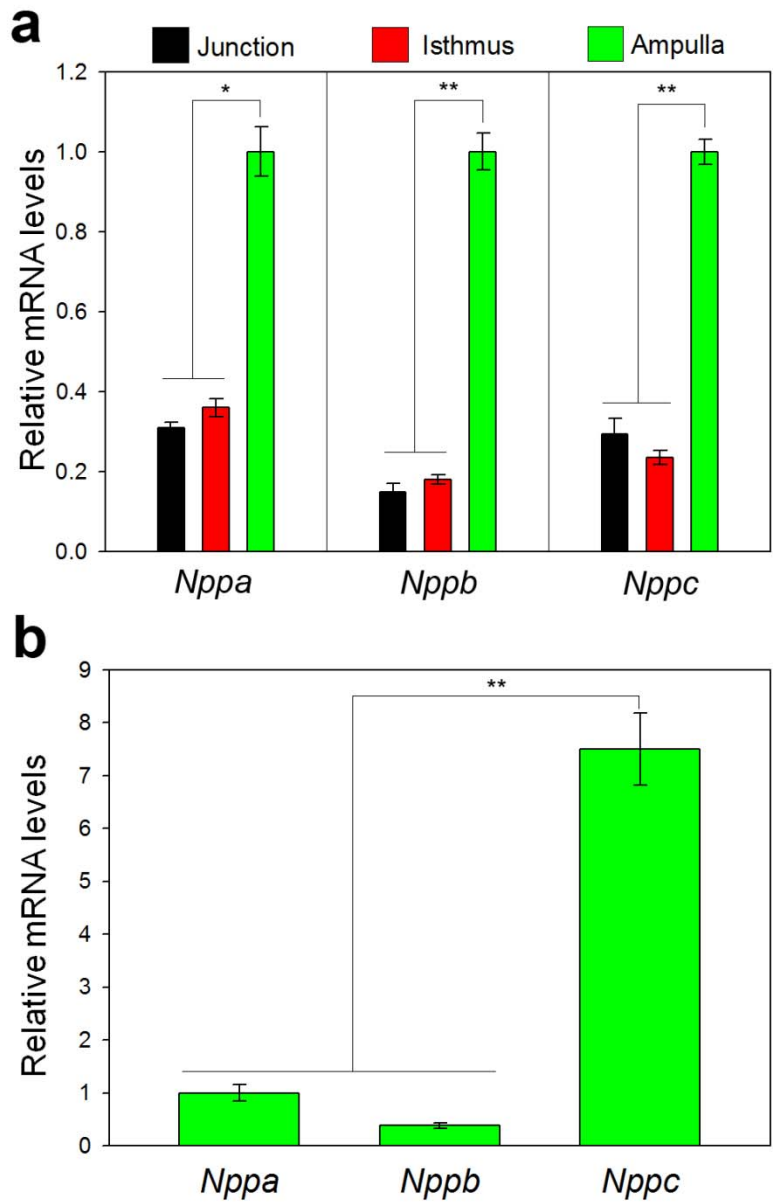
40	Species	Ligand	Amino acid sequence	Receptor	Signaling	Reference
41	<i>Arbacia punctulata</i>	Resact		A receptor-type guanylyl cyclase	cGMP	ref. 1
42						
43	<i>Asterias amurensis</i>	Asterosap		A single 130-kDa membrane protein	cGMP	ref. 2
44						
45	Mouse	NPPA		Natriuretic peptide receptor 1	cGMP	ref. 3, 4
46						
47	Mouse	NPPB		Natriuretic peptide receptor 1	cGMP	ref. 3, 4
48						
49	Mouse	NPPC		Natriuretic peptide receptor 2	cGMP	ref. 3, 4
50						
51						
52						

53 **References**

54 1 Kaupp, U. B. *et al.* The signal flow and motor response controlling chemotaxis of  
 55 sea urchin sperm. *Nat Cell Biol* **5**, 109-117 (2003).  
 56 2 Nishigaki, T., Chiba, K. & Hoshi, M. A 130-kDa membrane protein of sperm  
 57 flagella is the receptor for asterosaps, sperm-activating peptides of starfish  
 58 *Asterias amurensis*. *Dev Biol* **219**, 154-162 (2000).  
 59 3 Potter, L. R., Abbey-Hosch, S. & Dickey, D. M. Natriuretic peptides, their  
 60 receptors, and cyclic guanosine monophosphate-dependent signaling functions.  
 61 *Endocr. Rev.* **27**, 47-72 (2006).  
 62 4 Zhang, Y. *et al.* Porcine natriuretic peptide type B (pNPPB) maintains mouse  
 63 oocyte meiotic arrest via natriuretic peptide receptor 2 (NPR2) in cumulus cells.  
 64 *Mol Reprod Dev* **81**, 462-469 (2014).

65 **Fig. S2. *Nppc* mRNA is expressed predominantly in the ampulla of estrous mice.**  
 66 (a) Comparison of natriuretic peptides mRNA levels in the uterotubal junction  
 67 (Junction), isthmus and ampulla from the oviducts of estrous mice. The mean value in  
 68 ampulla group was set as 1. Bars indicate mean  $\pm$  SEM of four experiments. \* $P$  <  
 69 0.05; \*\* $P$  < 0.01. (b) Comparison of *Nppa*, *Nppb* and *Nppc* mRNA levels in the  
 70 ampulla collected from estrous mice. Bars indicate mean  $\pm$  SEM of four experiments.  
 71 \*\* $P$  < 0.01.

72  
73  
74  
75  
76  
77  
78  
79  
80  
81  
82  
83  
84  
85  
86  
87  
88  
89  
90  
91  
92



93

94 **Fig. S3. NPR2 is expressed in spermatozoon.** (a) Comparison of *Nppc* and *Npr2*  
95 mRNA levels in fresh spermatozoa. Bars indicate mean  $\pm$  SEM of three experiments.  
96 \*\*\* $P < 0.001$ . (b) Comparison of *Npr2* mRNA levels in fresh and capacitated  
97 spermatozoa. No obvious change was indicated. (c-e) Capacitated spermatozoa were  
98 incubated with 100 nM FAM-NPPC for 30 min, and the fluorescent ligand binding  
99 was assessed by a confocal laser-scanning microscope. Representative images showed  
100 fluorescence (c), bright (d) and merge (e) fields. Scale bars, 20  $\mu$ m. (f) Comparison of  
101 FAM-NPPC binding in fresh, capacitation and attraction spermatozoa. Bars indicate  
102 the mean  $\pm$  SEM of three experiments.  $n = 500$  for each group. \*\* $P < 0.01$ ; \*\*\* $P <$   
103 0.001.

104

105

106

107

108

109

110

111

112

113

114

115

116

117

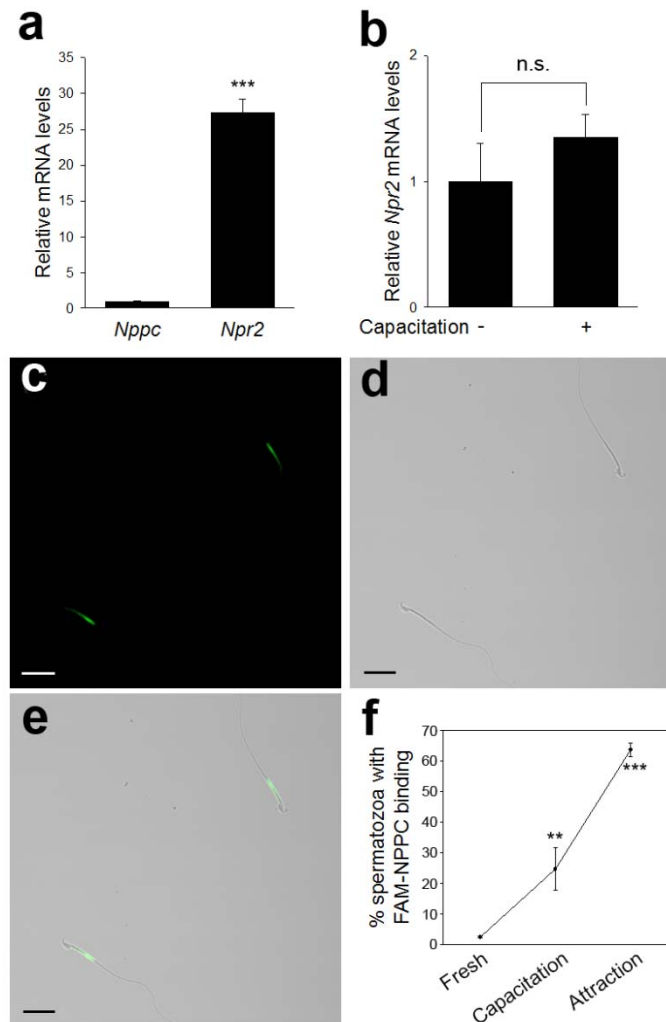
118

119

120

121

122



123

124 **Fig. S4. Failure in FAM-NPPC binding to spermatozoa from *Npr2* mutant mice.**

125 Capacitated spermatozoa from *Npr2* heterozygote and mutant mice were incubated

126 with 100 nM FAM-NPPC for 30 min, and the fluorescent ligand binding was assessed

127 by a confocal laser-scanning microscope. **(a-c)** Representative images showed

128 fluorescence **(a)**, bright **(b)** and merge **(c)** fields. Scale bars, 20  $\mu$ m. **(d)** Comparison

129 of FAM-NPPC binding in capacitated spermatozoa from *Npr2* heterozygote and

130 mutant mice. Bars indicate the mean  $\pm$  SEM of three experiments.  $n = 500$  for each

131 group. **\*\*** $P < 0.01$ .

132

133

134

135

136

137

138

139

140

141

142

143

144

145

146

147

148

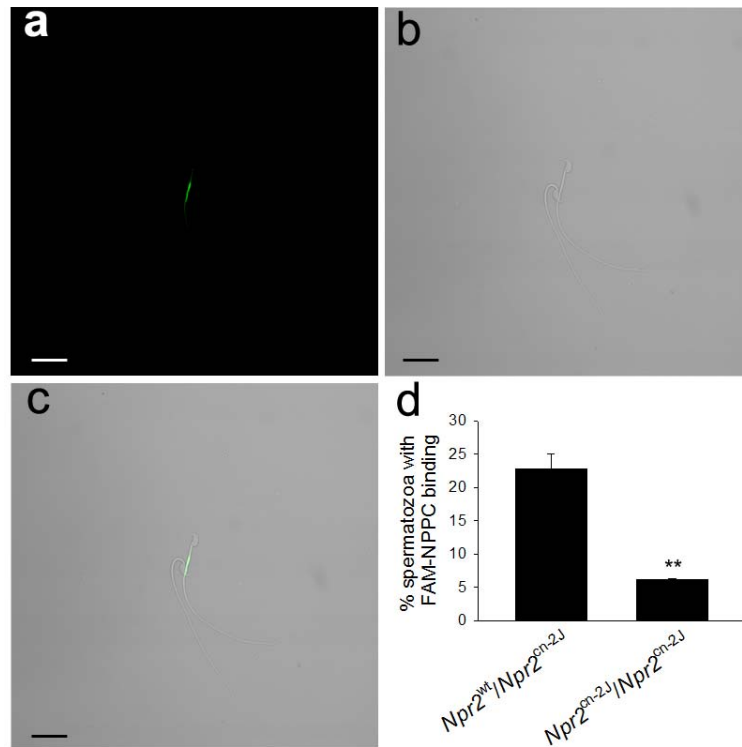
149

150

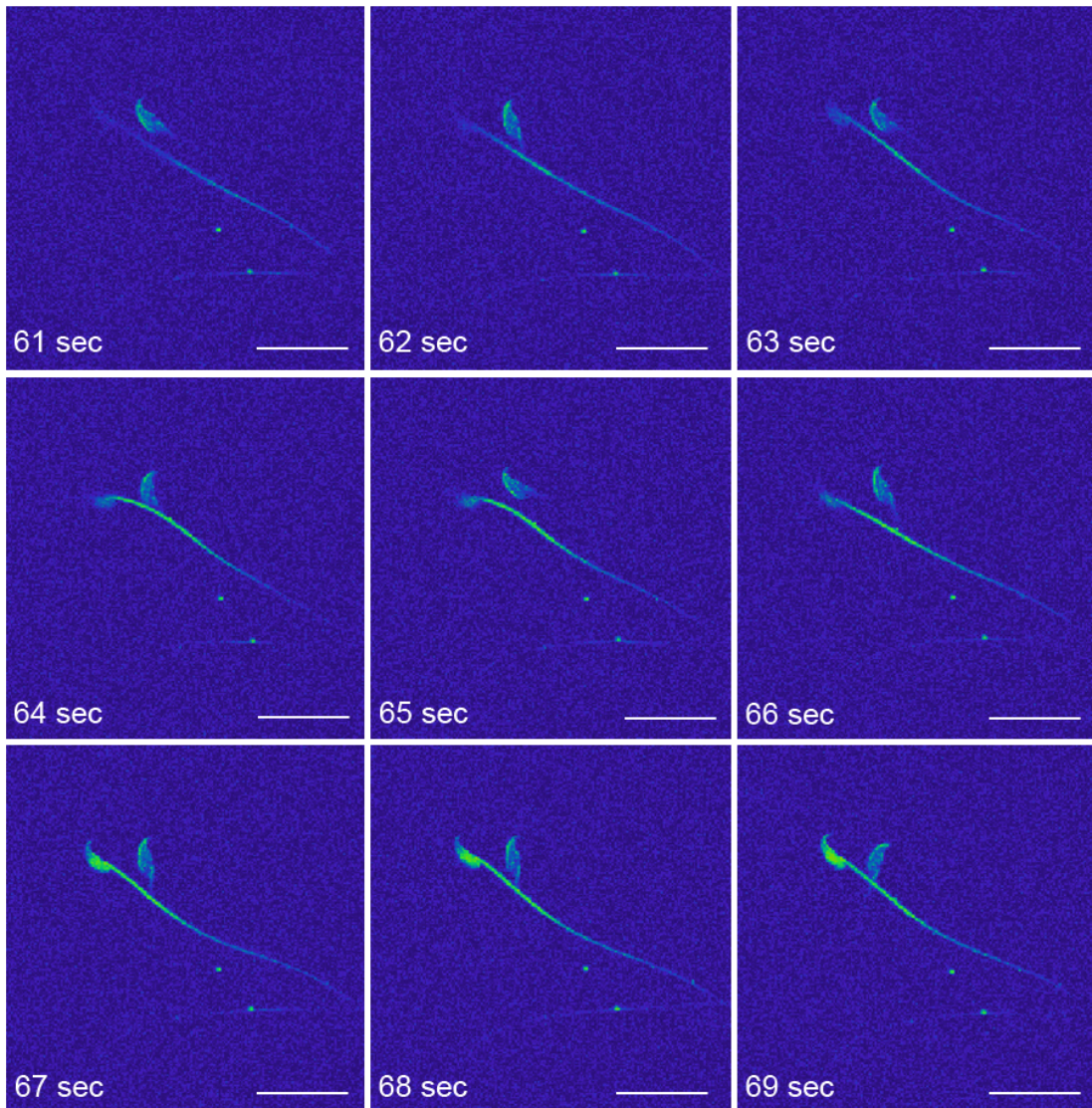
151

152

153



154 **Fig. S5. Time lag in the  $\text{Ca}^{2+}$  influx induced by NPPC between flagellar midpiece**  
155 **and head of mouse spermatozoon.** Time measurement analysis showing the  
156 propagation of elevated  $\text{Ca}^{2+}$  from the midpiece of flagellum to the head after  
157 application of 0.1 nM NPPC. The zero time was defined as the time of NPPC addition.  
158 Representative images are presented in a pseudocolor format. Scale bars, 20  $\mu\text{m}$ .





185 **Fig. S6. *l-cis*-Diltiazem blocked NPPC-induced sperm accumulation.** (a) Sperm  
186 accumulation in the capillaries in the groups of control, NPPC (0.1 nM),  
187 *l-cis*-Diltiazem (*l-cis*-D, 50  $\mu$ M) and NPPC + *l-cis*-Diltiazem. Bars indicate the mean  
188  $\pm$  SEM of three experiments. (b) Sperm accumulation in the oviductal ampullae. Bars  
189 indicate the mean  $\pm$  SEM of four experiments. \*\*\*  $P < 0.001$ .

190  
191  
192  
193  
194  
195  
196  
197  
198  
199  
200  
201

